Improvement of Linear Spectral Mixture Analysis and experimentation in Estimation of Urban Vegetation Fraction

Wenze Yue[1], Jianhua Xu [2], Jiawei Wu [2*]
(1. College of Southeast Land Management, Zhejiang University, Hangshou 310029; 2.Department of Geography, East China Normal University, Shanghai, 200062)

***Abstract*-Abundance of vegetation plays an important role in urban ecosystem, urban planning and development. Traditional classification methods on remote sensing data by assigning each pixel membership in one, and only one have the primary shortcomings of their inability to accommodate spectrally mixed pixels in gradational land covers. The traditional classification methods are giving way to spectral mixture analysis (SMA) gradually which is better in acquiring quantitative information for specific land covers. Vegetation fraction, in a general way, is defined as the areal fractions of vegetation within each pixel. This paper, besides introducing the traditional technique of SMA, discusses the improvement of traditional technique from the aspects of data noise removal, least-squares solution with constraining sum of endmembers fractions to unit, pixel purity index and the selection of endmembers. LSMA is tested further with the Shanghai city as an example. Unmixing pixels with root mean square (RMS) error less than 0.02 accounts for the proportion of 98.5%. The spatial distribution of vegetation is corresponding to actual situation. Then we conclude that: the improved LSMA is appropriate for estimating quantitative vegetation fraction and the technique will be widely applied in urban environment.**

I. INTRODUCTION

In the urban environment, both quality of life and biophysical processes are closely related to the presence of vegetation. Green vegetation is not only an important member of the urban/suburban landscape, but also an adjustor to ecosystem (e.g. reduce the effect of heat island in urban area). As an indispensable component to the residents, the distribution of green vegetation is placed on a more and more important status. For describing vegetation quality and indicating ecosystem change, the vegetation fractional coverage is an important parameter [1-3]. Spectral mixture analysis (SMA) has been frequently used to derive subpixel vegetation information from remotely sensed imagery in urban areas. The core of vegetation fraction calculation is unmixing pixels, That is, how to select appropriate vegetation endmember and resolve its spectral fraction in each pixel is very important. Here, vegetation fraction (abundance) must be understood completely, which in a general way, is defined as the areal fractions of vegetation within each pixel. On the problem many studies and methods have been conducted [4]. In the paper, how to generally improve accuracy of results was discussed on the basis of experiment in Shanghai city in China.

Author's information: Funded by National Nature Science Foundation of China (NSFC): 40371092. *: Corresponding author, Tel.: +86-21-62233861; Fax: +86-21-62232416. E-mail address: yuewenze@163.com

II. THEORY

Linear spectral mixture analysis (LSMA) is an image processing method, which assumes that spectrum measured by a sensor is a linear combination of the spectra of all components within the pixel [5]. The mathematical model of LSMA can be expressed as [3]:

$$R_i = \sum_{k=1}^{n} f_k R_{ik} + ER_i \quad (1)$$

Where $i = 1,...,m$ (number of spectral bands); $k = 1,...,n$ (number of endmembers); R_i is the spectral reflectance of band i which contains one of more endmembers; f_k is the proportion of endmember k within the pixel; R_{ik} is the known spectral reflectance of endmember k within the pixel on band i; and ER_i is the error for band i. A constrained least-squares solution was used in this research, assuming that the following two conditions are satisfied simultaneously:

$$\sum_{k=1}^{n} f_k = 1 \text{ and } 0 \le f_k \le 1 \quad (2)$$

Estimation of endmember fraction images with LSMA involves (1) image processing, (2) endmember selection, and (3) unmixing solution and evaluation of fraction images. Of these steps, selecting suitable endmembers is the most critical one in the calculation of high quality fraction images.

III. STUDY AREA AND DATA DESCRIPTION

The study area, aiming at Shanghai, which is the biggest city in China (Fig.1), This region is one of the fastest growing areas in East China.

The data used in this study was a Landsat Enhanced Thematic Mapper plus (ETM+) scene, dated on 14 June 2000. The digital numbers (DNs) were converted to normalize exo-atmospheric reflectance measures. No atmospheric corrections were performed. Error with geometric correction is less than one pixel (30m).

IV. ESTIMATION OF VEGETATION FRACTION

A. Data Transformation

One approach for choosing image endmembers is selecting representative homogeneous pixels from satellite images through visualizing spectral scatter plots of image band

combinations. In this test, to concentrate information of original image into relatively less band combinations, the minimum noise fraction (MNF) procedure embedded

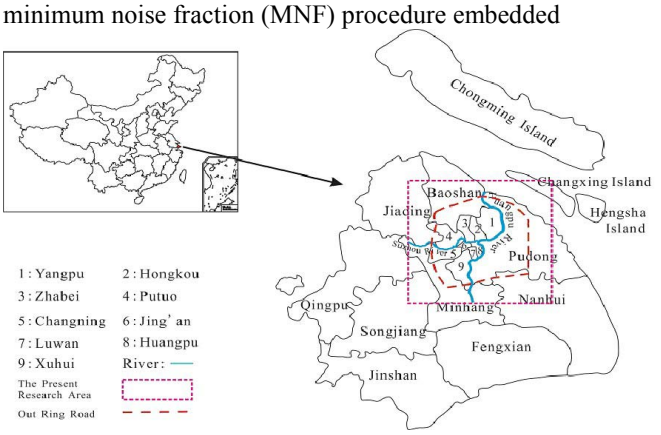

Figure 1. Shanghai city at the estuary of Yangtze River.

in software ENVI was applied [6]. The first three MNF components provide primary information of the original ETM+ image. Higher order MNF components, show diminishing spatial coherence and provide little information. It can be concluded that first three, especially the first two components, can determine our image dimensionality. The distribution of the transformed reflectance within the three-dimensional feature space corresponding to the low-order MNF dimensions suggests that the observed reflectance might be described by a three-component mixing model.

B. Pixel Purity Index Algorithm

A hyper spectral image is a two-dimensional array of hyper pixels. These elements can be viewed as vectors of D data, each of which representing a specific value for a given wave length among hundreds of spectral bands. The assumption in LSMA is that a hyper image contains relatively few materials and pure materials (endmembers) are mixed into hyper pixels. The pixel purity index (PPI) is used to find the most "spectrally pure", or extreme, pixels in multispectral and hyperspectral images [7]. The most spectrally pure pixels typically correspond to endmembers, so that all the remaining pixels can be expressed as a linear combination of them. The pixel purity index is computed by repeatedly projecting each data point in n-dimensional scatter plots onto a random unit vector (Fig.2). The extreme pixels in each projection are recorded and the total number of times each pixel marked as extreme is noted to be the index.

A pixel purity index image is created in which the DN of each pixel corresponds to the number of times that pixel was recorded as extreme. A mask gained from the PPI image was used to filter "pure pixels" in which endmembers were selected.

C. Selection of Endmembers

First three MNF components, which were projected to two-dimension, formed scatter plots shown in Fig.3. Density-shaded scattergrams appearing like a triangle whose corners obviously contain endmembers suggest a good fit for linear combinations of three endmembers. Figure of eigenvalues distribution at the low corner on right of Fig.3 tells us that most information of the original imagery can

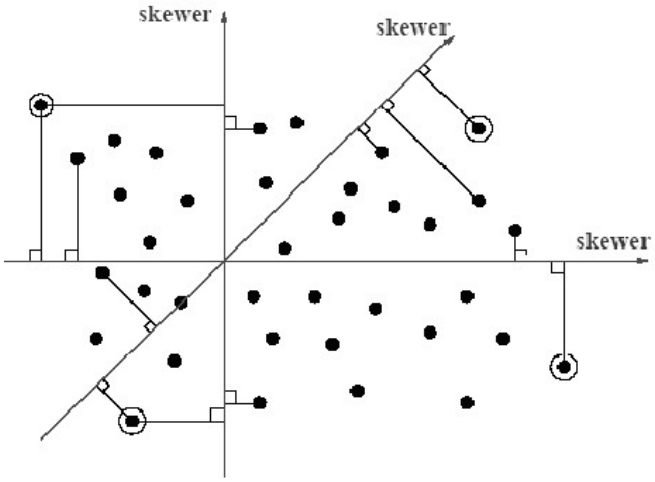

Figure 2. Schematic view of scatters, which were projected to random skewers in 2D space

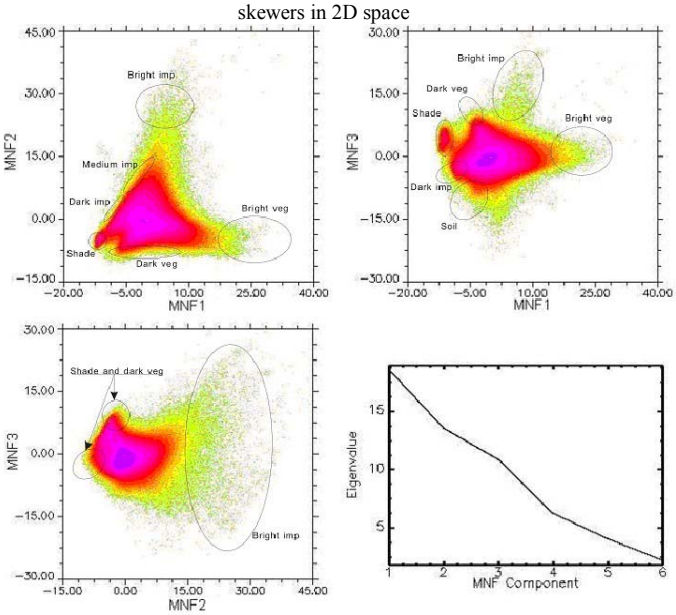

Figure 3. Pixel scatter plots with different combinations of the first three MNF components.

be revealed by MNF band 1, MNF band 2 and MNF band 3. A divarication on the left low corner in scatter plot between MNF1 and MNF2 still falls into the fact that at the time of imaging, paddy was just planted. These areas show a reflectance feature between water and vegetation. Meanwhile, apexes in the scatterplots of MNF1 and MNF 3 as well as MNF2 and MNF3 can also represent spectral features of distinctive land covers well.

Carrying on the result, which was made of PPI after masking, taking MNF1, MNF2, MNF3 as reference frame, each pixel, was complied into stereograph. All pixels that meet PPI qualification behave like a polyhedron over all (Fig.4). High albedo endmember is of the most disperse spectral feature, so it takes up two corners. On the Basis of discussion above, three endmembers can represent the urban surroundings including high albedo endmember such as glass,

new concrete surface; low albedo endmember such as river surface, shade, asphalt; and vegetation as an individual endmember. At this point, with the interaction with original image, one hundred points for each endmember were selected at the corners of polyhedron. The method is also similar to the

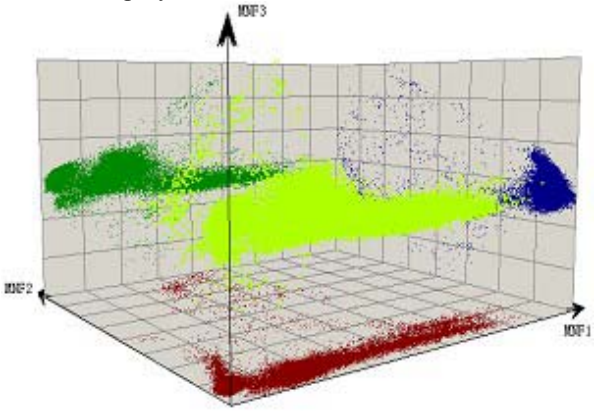

Figure 4. Pixel scatter plot in 3D space of MNF1~3

minimally inclusive feature space selection in the scattergram of MNF bands 1 and 2; however, our process was performed in the three-dimensional mixing space. The average reflectance vectors of endmembers selected above were specified to each ETM+ bands range shown as Fig.5. Polluted atmosphere may express some reasonable explanation such as the less obvious 'red edge' phenomena of vegetation.

V. Results And Discussion

A. Results

A least square constrained method was applied to formula (1) to get the fraction image of vegetation [8]. It shows a high correlation between the vegetation fraction image (Fig.6) and the actual vegetation abundance in Shanghai. Besides the water bodies, vegetation fraction calculated from pixels is almost lower than 10% along with both sides of Suzhou river from the east of People Square in the center of the city. High vegetation fraction values appear on the green belt or parks such as New Jiangwan Town, Youthful forest park and Changfen Park whose values arrive to higher than 60%. As a whole, vegetation fraction shown in the Fig.6 grows larger and larger from the center to periphery, the belt around out ring road. There is a belt whose value is between the out ring road and the old urban area, especially in Nanhui zone and Jiading zone, where much little crop was growing.

B. Root Mean Square (RMS) errors

During the process of "unmixing pixels", as errors are inevitable, ofen from the data preparation, endmembers quantitative determination and selections and inversion of the linear mixing model by least square solutions restrict the accuracy of vegetation fraction, RMS misfits were adopted to validate vegetation fraction:

$$RMS = \sqrt{(\sum_{i=1}^{m} ER_i^2)/m} \quad (3)$$

The maximal RMS error is 0.0867. Most of RMS error are lower than 0.01 according to RMS frequency histogram (Fig.7). 98.5% of RMS errors are smaller than 0.02, which shows a better result than former studies [3]. The distribution of RMS is not symmetrical. As a whole, the values located in urban area are higher than in suburb, and in the old city zone are also higher than in newly built city zone. Comparatively, mixed pixels are more inclined to have large RMS errors than pure pixels. The more complicated inside the mixed pixel, the larger RMS error is, which suggests there may be another

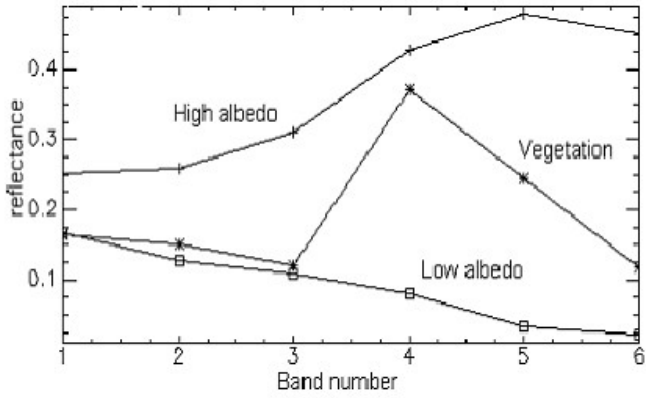

Figure 5. The reflectance of three spectrum endmembers at six bands

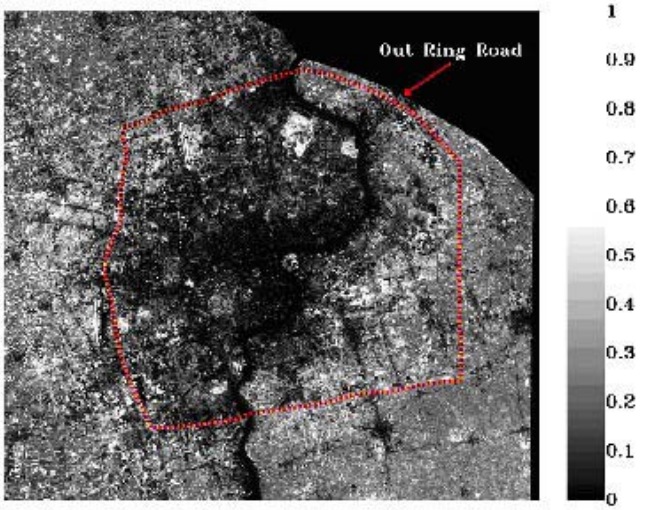

Figure 6. Vegetation fraction images of Shanghai surrounding area

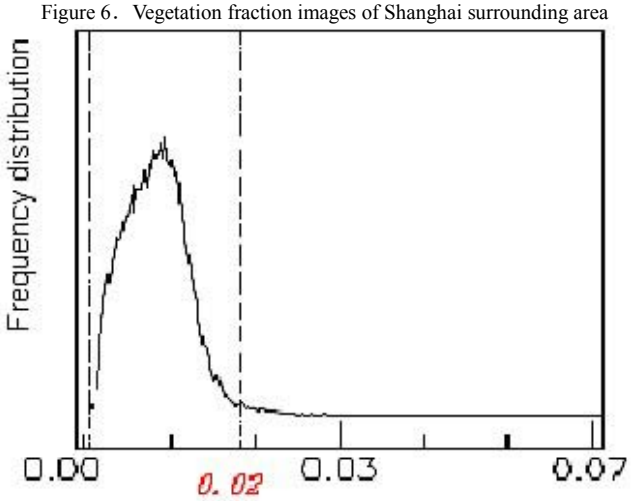

Figure 7. The image and frequency plot of root mean square.

spectral endmember to be further studied.

C. Application

15 high-resolution color aerial photographs, adjusted to the same coordinate as ETM+, were singled out from 253 photographs taken for whole city of Shanghai in 1998 to analyze our results. 174 sample areas were sorted out. The functions such as overlay and zonal statistics embedded in software ARCGIS were applied to analyze the vegetation fraction distribution based on different sample types, the results are showed in Table Ⅰ.

TABLE Ⅰ:

The statistic values of vegetation fraction associated with sample categories.

type	count	area	min	max	range	mean	STD
Farmland	18	571500	0.0829	0.7433	0.6604	0.3542	0.1553
Grass	47	368100	0.0103	0.8062	0.7959	0.5787	0.1315
Roads	17	233100	0.0000	0.2619	0.2619	0.1004	0.0498
Woods	46	260100	0.2656	0.7400	0.4744	0.5080	0.1083
Water	14	430200	0.0000	0.3071	0.3071	0.0381	0.0527
Residuals	32	648000	0.0000	0.4592	0.4592	0.0426	0.0479

From Table Ⅰ, first of all, the minimum value Zero appears in such areas as road, water and residence, which suggests there is nearly no vegetation land cover. The minimum values appearing in farmlands, grasslands and woods are all over zero, while the maximum value in all these minimum values rising to 26.56% emerges in areas of woods, which can be explained by the fact that in urban area, woods are almost composed of high density sylvan parks and nurseries. When it comes to the maximum values, grasslands mainly including artificial greenbelts and lawns take the first place by 80.62% in all land covers. Woods and farmlands with the limitation of row spacing to grow better, however, reach to 74% and 74.33%. The maximum values for road, water and residential areas are much smaller than others, especially for residential areas only 45.92%. In general, the values vary with the variation of sample areas, and the range of the values reflects the difference inside sample areas.

The mean of artificial grasslands and lawns shows the highest value of 57.87%. Woods takes the second place by the value of 50.80% while the farmland 35.42% for diversity in crop's green quantity. The last three sample areas obviously show a low value in that no green vegetations were located there. Shape of road may affect selecting sample areas from other adjacent land covers; in addition, influence may result from the green trees along with the road. For this reason, road's vegetation fraction mean comes to 10.04%. Residential areas show the average value of 4.26%. Water bodies in Shanghai mainly containing rivers and lakes, although impacted by the phytoplankton and redundant nutrition, have a lowest value of 3.81%. When comes to the standard deviation, farmlands are most arrestive with the explanation of planted paddy different from vegetable. Water bodies, roads and residential areas have both low vegetation fractions and small standard deviations.

VI. CONCLUSIONS

This paper draws conclusions as follows:

(1) MNF transformation not only reduces data redundancy and correlations between spectral bands, but also concentrates the information of high signal-noise ratio to the first several components. This ensures that most information can be revealed in fewer bands than un-transformed data.

(2) PPI is introduced to help to select endmembers and limit the extent of endmember selection. By mask from PPI image, the first three MNF components are compiled to form three-dimensional mixing space. By expanding the two-dimensional mixing space to a three-dimensional mixing space, since a third component is considered, the selection of endmembers will undoubtedly improve the result's accuracy.

(3) With the application of vegetation fraction in Shanghai, different land covers take on different mean vegetation abundance: farmlands accounts for a mean value of 35.42%; grass lands 57.87%; roads 10.04%; woods 50.80%; water 3.81%; residence 4.26%.

REFERENCES

[1] R. J. Kauth, G. S. Thomas, "The tasseled cap—a graphic description of the spectral-temporal development of agriculture crops as seen by Landsat," *Proceedings of the Symposium on Machine Processing of Remotely Sensed Data*, pp.4041-4051, 1976.

[2] C. Small, "Estimation of urban vegetation abundance by spectral mixture analysis," *Int. J. Remote Sens.*, vol.22, No.7, pp.1305~1334, 2001.

[3] C. Small, "Multitemporal analysis of urban reflectance," *Remote Sens. Environ.,* vol.81 pp.427~442, 2002.

[4] Conghe Song, "Spectral mixture analysis for subpixel vegetation fractions in the ureban environment: How to incorporate endmember variability?," *Remote Sens. Environ.*, vol.95, pp.248-263, 2005.

[5] Adams, J. B., Smith, M. O., & Gillespie, A. R. Imaging spectroscopy: Interpretation based on spectral mixture analysis. In *C. M. Pieters, & P. Englert (Eds.), Remote Geochemical Analysis: Elemental and Mineralogical Composition*. New York, Cambridge Univ. Press, 1993, pp.145-166.

[6] A. A. Green, M. Berman, & P. Switzer, et al., "A transformation for ordering multispectral data in terms of image quality with implications for noise removal," *IEEE Trans. Geosci. Remote Sensing*, vol.26, No.1, pp.65-74, 1988.

[7] J.W. Boardman, F. A. Kruse, and R. O. Green, "Mapping target signatures via partial unmixing of AVIRIS data," in *Summaries, Fifth JPL Airborne Earth Science Workshop*, JPL Publication, 1995, pp.23-26.

[8] Y. E. shimabukuro and J. A. Smith, "Least squares mixing models to generate fraction images derived from remote sensing multispectral data," *IEEE Trans. Geosci. Remote Sensing*, vol.29, pp.16-20, 1991.